



Rainfall-runoff modeling using HEC-HMS model in an ungauged Himalayan catchment of Himachal Pradesh, India

C Prakasam^{1,2} · Ravindran Saravanan^{1,3} · Deepesh Machiwal⁴ · Mukesh Kumar Sharma⁵

Received: 31 May 2022 / Accepted: 27 May 2023 / Published online: 14 June 2023
© Saudi Society for Geosciences and Springer Nature Switzerland AG 2023

Abstract

Assessment of environmental flow, that has to be maintained along a waterway to keep up health of riverine biological systems, is a key challenge in alleviating impact of establishing hydropower projects especially in mountainous ungauged catchment under limited data conditions. This study addresses the data scarcity issue by prediction of runoff from a Himalayan catchment, India, using HEC-HMS model and then estimating environmental flow based on daily rainfall data of 39 years (1980–2018). The soil conservation service–curve number method is employed for surface runoff estimation that utilizes spatially distributed maps of soil types, drainage, stream order, 4-year land use/land cover (1990, 2000, 2010, and 2020), and hydrologic soil group (HSG). Steep slopes (more than 60%), high annual rainfall (1377 mm), large area under C class of HSG (477.94 km²), and moderate values of curve number (70.51, 70.36, 70.16, and 70.54) revealed high potential for surface runoff generation in the catchment. Predicted runoff depicted a gradually increasing trend during 1980–1995 and decreasing trend during 1995–2008 and 2011–2017. In addition, an abrupt change was observed in annual runoff values in years 1992, 1998, and 2018 when the peak rate of runoff crossed the value of 2000 m³ s⁻¹. The HEC-HMS model is validated by close agreement between peaks and troughs of runoff and rainfall values, and with reasonable values of correlation coefficient (0.57) and coefficient of determination (0.33). The annual values of environmental flow is obtained as 75 and 55 m³ s⁻¹ from the flow duration curves at 70th and 90th percentiles, respectively. Findings of this study are useful for management of flood water in other ungauged mountainous catchment of Himalayan region as well as in other parts of the world under data scarcity conditions.

Keywords Data-scarcity condition · Environmental flow · HEC-HMS model · Mountainous catchment · Rainfall-runoff model · Ungauged catchment

Introduction

Rainfall and runoff are two vital components of hydrologic cycle where excess of the rainfall, after infiltration and evaporation, along with climatic, physiographic, and geologic conditions determines the generation of the runoff in a

catchment (Seibert 1999). Estimation of runoff is important for solving a variety of catchment management problems such as dealing with flood mitigation, storm water management, rainwater harvesting, and conservation, among others (Anandharuban et al. 2019). On the other hand, surface runoff in cultivated lands erodes topsoil and transports

Responsible Editor: Broder J. Merkel

✉ Deepesh Machiwal
dmachiwal@rediffmail.com

C Prakasam
cprakasam@gmail.com

Mukesh Kumar Sharma
mks.nihr@gov.in

¹ Department of Civil Engineering, Chitkara University, Himachal Pradesh, Solan, India

² Department of Geography, School of Earth Sciences, Assam University, Diphu Campus, Diphu, Karbi Anglong Assam-782462, India

³ Ecofirst Services Limited, Tata Enterprise, Bangalore, Karnataka, India

⁴ Division of Natural Resources, ICAR-Central Arid Zone Research Institute, Jodhpur, Rajasthan 342003, India

⁵ Environmental Hydrology Division, National Institute of Hydrology, Roorkee, Uttarakhand, India

nutrients to downstream depending upon type of cover crops and causing reduction in crop yields (Machiwal et al. 2021). In such a condition, knowledge about runoff process helps in regulating runoff quantities safely from field outlet and aid in agricultural water management. Runoff process, being highly dependent upon the rainfall, is generally simulated by hydrologic models. In hydrology, several types of models have been developed over the years for estimation of runoff or streamflow, which are categorized into three categories (Sharma and Machiwal 2021): (i) physical or process-based models, (ii) conceptual models, and (iii) black-box models. The physical or distributed/semi-distributed parameter models, based on analytical solutions of differential equations describing the physical laws of mass, energy, and momentum conservations, are capable of simulating the runoff accurately. However, these models require extensive field data, which are usually not available for the hilly catchments. Therefore, conceptual or lumped-parameter models being relatively simple and requiring fewer data have a great scope for their utilization in hilly catchments.

Modeling rainfall-runoff process in the mountainous terrain serves the purpose of overall assessment of the catchment response as a part of strategic planning to flood water management. In fact, modelers confront with the biggest difficulty of choosing a suitable rainfall-runoff model that is capable enough to simulate a wide range of runoff peaks or floods in the mountainous catchment especially under the absence of any gauging station and condition of limited data availability (Azmat et al. 2016). In general, selection of a feasible model depends on the basin characteristics and the goal behind runoff estimation in a catchment (Hunukumbura et al. 2008). It is seen that many recent studies employed semi-distributed models demanding large data to simulate the rainfall-runoff response in small catchments of semi-arid regions. In data-sparse conditions, physical hydrologic models demanding large data reveal a large uncertainty (Leimer et al. 2011), which makes the estimation of flood hydrograph even more difficult in ungauged catchments.

The runoff estimation remains a pressing task for the hydrologists in ungauged hilly catchments, which is also the case with most of the catchments in the Himalayan region due to rugged terrain (Sivapalan et al. 2003). In Himalayan catchments, monitoring of hydro-meteorological processes is also challenging as it is not feasible to measure hydrologic parameters in every small size catchment and at every location of a stream despite the fact that these catchments have a vast potential for hydropower development (Khatri et al. 2018). Nonetheless, runoff modeling has a greater significance for assessment of water availability in such data-scarce mountainous catchments for design, planning, operation, and management of hydropower projects. Hence, simplified and easy-to-use lumped-parameter models are used for runoff modeling in mountainous catchments under the data-limiting

conditions. It is further revealed that snowmelt contribution to runoff in the mountainous Himalayan catchments makes it further difficult for the hydrological models to simulate the runoff adequately (Khatri et al. 2018). Hence, only those hydrological models that have option for snowmelt runoff simulation such as Hydrologic Engineering Center–Hydrologic Modeling System (HEC-HMS), developed by the US Army Corps of Engineers (Feldman 2000), are useful in the mountainous catchments (Guo et al. 2015), and the same have been used to simulate runoff in hilly catchments in different parts of the world (e.g., Yilmaz et al. 2012; Gyawali and Watkins 2013; Rezaeianzadeh et al. 2013; Joo et al. 2014; Pokhrel et al. 2014; Azmat et al. 2017; Khatri et al. 2018; Kumar and Bhattacharjya 2020; Akinwumi et al. 2021).

The HEC-HMS model has been successfully used for simulating rainfall-runoff process in ungauged Koraiyar River basin in Tiruchirappalli city region, India (Natarajan and Radhakrishnan 2021). The HEC-HMS model calibrated and validated using the flood event data of 1999 measured at the outlet of the basin as Koraiyar River basin did not have a continuous record of flow measurements and only extreme flood events were recorded. Rao (2020) analyzed runoff potential in the ungauged upper Gosthani River basin located in the Visakhapatnam district of Andhra Pradesh, India, using SCS-CN method. Results revealed that the mean annual runoff in the basin was estimated to be 454.9 mm, which corresponded to 40.6% of the mean annual rainfall. In two ungauged sub-quaternary catchments, i.e., Tshiluvhadi and the Nzhelele Rivers of the Nzhelele River catchment in the Limpopo River basin of South Africa, the modified nearest neighbor regionalization approach was applied to generate natural streamflows and environmental flows using Mike 11 and Australian water balance model (Makungo et al. 2010). The streamflow hydrographs simulated from both the models were found comparable and showed behavior similar to that reported in earlier studies. van Emmerick et al. (2015) proposed an alternative method for validating the hydrologic behavior of Chamcar Bei, a small-scale and ungauged irrigation system in Cambodia, by collecting data of annual patterns of river discharge, runoff mechanisms, and minimum and maximum reservoir levels by interviewing 20 farmers. Ditthakhit et al. (2021) evaluated three regression-based and two distance-based regionalization methods to determine regional parameters in rainfall-runoff model for three major river basins of Thailand, i.e., Peninsula-East Coast, Peninsula-West Coast, and Thale Sap Songkhla. Results of Taylor's graphical diagram indicated that random forest provided the parameter values closest to rainfall-runoff model, followed by spatial proximity approach, M5 model tree, physical similarity approach, and multiple linear regression.

However, such studies are lacking in high-altitude mountainous catchments of Himachal Pradesh (India)

having some portion of land inaccessible and are known for hydropower production. Many hydropower plants have been designed and established in the area; however, their environmental impacts are often overlooked in their construction and operation. In order to alleviate the worsening impact of hydropower plants on the environment, provision of environmental flow is suggested as a mitigation strategy. Computation of environmental flow depends upon the data of surface flow or runoff potential, which is usually not available for the ungauged rugged catchments. Therefore, this study was undertaken with two objectives: (i) to estimate runoff or inflow for Larji dam situated in Kullu district of Himachal Pradesh using HEC-HMS model based on rainfall data, and (ii) to evaluate environmental flow using the estimated inflow data. The findings of this study would be useful in understanding hydrological response of similar ungauged catchments in mountainous Himalayan region.

Study area description and data collection

Larji dam is situated on the Beas River in Kullu district of Himachal Pradesh, India. The catchment of the dam is spread over an area of 4921 km² and is located from 31°31' N to 32°10' N latitude and from 76°56' to 77°50' E longitude at an altitude of 2299 m above the mean sea level. The location map of the study area is shown in Fig. 1. The dam is constructed for generating hydro-electric power with 126 MW installed capacity. The live storage capacity of the Larji reservoir is 230 ha m, which is adequate for running the power station at full installed capacity for more than 4 h a day during lean periods. Precipitation in the study area is mainly received from the southwest monsoon as well as due to the western disturbances that pass over northwest part of India during winter. The southwest monsoon generally lasts from June to September and may sometimes extend

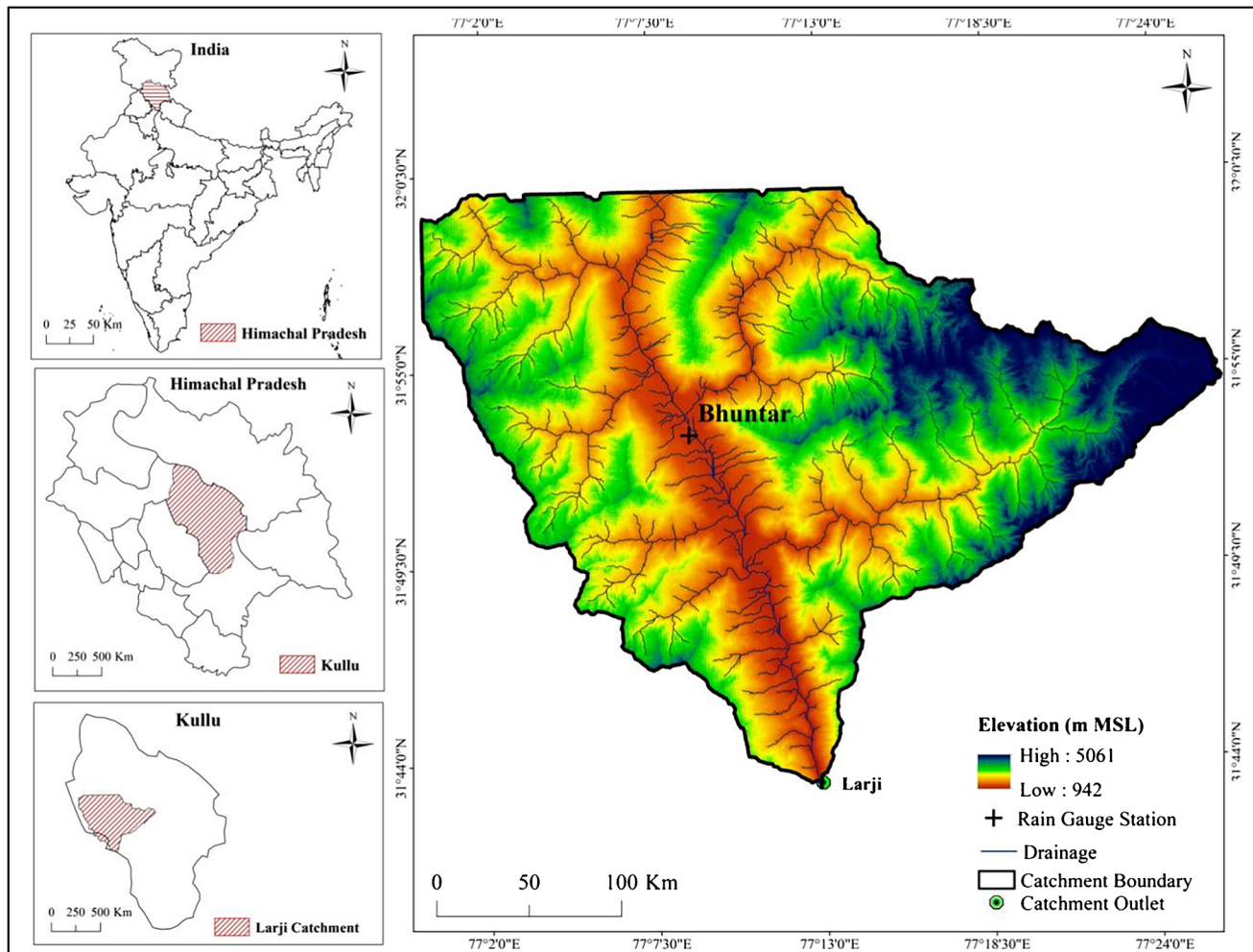


Fig. 1 Location map of the study area (Larji catchment) showing land elevation and drainage network prepared using ASTER-Digital Elevation Model

up to October. Precipitation during the northwest monsoon is usually not heavy, but sometimes it may contribute significantly toward flood runoff. On the other hand, winter precipitation occurs as either rain or snow depending upon the altitude and meteorological conditions. This rainfall does not directly contribute to river discharge rather mostly goes to feed snow-covered areas of the catchment. The average annual rainfall of the area is 1377 mm, ranging from 63 in January to 344 mm in July month. Low elevation lands of Kullu district experience hot summer with temperature rising up to 40 °C and cold winter with frost and fog. The average annual temperature for the area is 16.1 °C. Due to various developmental activities like construction of the road, water supply schemes, etc., soil erosion takes place at a high-level from Manali to Kullu and from Manali to Palchan (Prasad et al. 2016).

In this study, daily precipitation data were collected for three raingauge stations, i.e., Bhuntar (31°53'02.3"N 77°08'40.8"E), Sundernagar (31°31'56.2"N 76°53'33.3"E), and Dharamsala (32°12'57.4"N 76°19'09.5"E), from the India Meteorological Department (IMD), Shimla, Himachal Pradesh, for the past 39 years (1980–2018). Daily rainfall series were converted to monthly and annual series for further analysis. Digital elevation model (DEM) from ASTER at 30-m spatial resolution was downloaded for the catchment from the earth explorer website (<https://earthexplorer.usgs.gov/>). A total of four satellite imageries for the years 1990 (Landsat 1-5 MSS), 2000 (Landsat 7 ETM+), 2010 (Landsat 7 ETM+), and 2020 (Landsat 8 OLI/TIRS) were downloaded from the earth explorer website (earthexplorer.com) and used to develop land use/land cover maps of the study area. The imageries were chosen for the particular days when there was less than 5% cloud cover. Details of the acquired imageries are summarized in Table 1. Soil map of the study area (9th Edition, 2003) was collected at the scale of 1:50,000 from the Soil and Land Use Survey of India (SLUSI), Indian Agricultural Research Institute, PUSA, New Delhi.

Materials and methods

Preparing drainage and slope maps for delineation of dam catchment

The DEM of the study area was imported into geographic information system (GIS) and was used for delineating the catchment of the dam. Prior to catchment delineation, the DEM was processed for filling up voids, followed by computation of flow direction and flow accumulation using GIS. The processed DEM for the upstream side or catchment of the dam is shown in Fig. 1. In GIS, drainage was derived using criterion of flow accumulation value greater than 1000 for every pixel of the DEM. The processed DEM was utilized to generate flow direction and accumulation maps, which were subsequently used to generate drainage and stream-order maps of the study area. Order of a stream is proportion of the overall size of a stream and the smallest of tributaries, generally enduring are alluded to as first-order streams (Strahler 1957). Slope map helps understanding runoff retaining capacity. A second-order stream begins from a point where two 1st orders meet, and it is continued until the water exhausts into another significant stream. Drainage density, representing proportion of total length of the streams to a given area and indicating closeness of spacing of channels of an area (Haan 2002), was also computed. The catchment was then clipped from the upstream-side drainage map using four-point algorithm with reference to location where the dam was situated. The dam location was considered outlet of catchment and was imported into GIS from Google Earth image. All GIS-related operations were performed using ArcGIS 10.3.

Analyzing rainfall statistics

Basic statistical properties, i.e., mean, standard deviation, coefficient of variation, skewness, and kurtosis, were computed for 39 years (1980–2018) monthly and annual series of three rain gauge stations, i.e., Bhuntar, Sundernagar, and

Table 1 Details of acquired satellite imageries used in the study

Items	Particulars			
	1990	2000	2010	2020
Date of imagery acquisition	23-10-1990	22-11-2002	17-11-2011	28-10-2019
Type of Landsat satellite	Landsat 1-5	Landsat 7	Landsat 8	Landsat 8
Landsat sensor	Multi-spectral scanner system (MSS)	Enhanced thematic mapper plus (ETM+)	Operational land imager/Thermal infrared sensor (OLI/TIRS)	Operational land imager/Thermal infrared sensor (OLI/TIRS)
Could cover (%)	< 5	< 5	< 5	< 5
Imagery download date	12-02-2023	12-02-2023	12-02-2023	12-02-2023

Dharamsala. Bar charts of monthly rainfall and box-whisker plots of the annual rainfall were also drawn to explore variability of rainfall series. Box-whisker plots summarize five statistical properties of a time series, i.e., minimum, maximum, median (50th percentile), non-outlier range (25th and 75th percentiles), and outliers (Machiwal and Jha 2012).

The weighted mean rainfall of the three stations was computed for further use in runoff modeling. Location of three rain gauge stations was imported in GIS and representative areas of three stations in the catchment were identified using the Thiessen polygon method. Relative weights of three stations were obtained as 0.572, 0.405, and 0.23, respectively, for Bhuntar, Sundernagar, and Dharamsala stations, which were multiplied by rainfall data of the corresponding stations and summed over the years to derive the mean values of monthly and annual rainfall series.

Development of land use/land cover map

The land use/land cover (LULC) helps identifying curve number that plays an important role in runoff generation. In this study, LULC maps of Larji catchment were developed for 4 years, i.e., 1990, 2000, 2010, and 2020, using satellite imageries of Landsat satellite. Of the total 11 bands of Landsat 8, eight bands have 30-m spatial resolution, one band has 15 m, and other two bands have 100-m resolution. A composite of six bands (bands 1 to 6) of Landsat 8 data was made using image analysis tool in GIS platform. The composited Landsat images were classified into different LULC classes using supervised classification. In supervised classification, the maximum likelihood classifier method was used for image classification. A training set of signature pixels for each class was created to classify all pixels of the Landsat image into identified LULC classes. The training set for each class had more than 50 pixels. The developed LULC maps were visually compared with Google Earth images of the area and toposheet accompanied by visiting a few sites in the area for verifying the accuracy of the LULC maps.

Preparing maps of hydrologic soil groups and curve number

The soil map of Larji catchment was used to create GIS-based hydrologic soil group (HSG) map depending upon soil characteristics, e.g., texture, depth, and infiltration properties. The soil map of the study area was digitized and clipped using the ArcGIS for the upstream side of the study area. Broadly, soil of the study area may be classified as coarse loam and fine loam with a major difference in their clay proportion. The coarse loam soil consists of 0–18% clay proportion with soil textures of sandy loam and loam, whereas the fine loam soil includes proportion of clay as 18–35% with textures of fine sandy, sandy clay loam, loam,

clay loam, and silty clay loam. The depth of the soil is classified as shallow (11–25 cm), deep (51–100 cm), and very deep (more than 100 cm) following the criteria used by Soil and Land Use Survey of India (SLUSI), New Delhi, India. The moisture content is notified in the area by Mesic soil. The moisture is either wet or dry, and a well-balanced. The final classifications are Typic Udorthents, Typic Eutrudepts, Lithic Hapludolls, and Typic Hapludolls in the study area.

After preparation of HSG and LULC maps, curve number (CN) was estimated for each unit of the sub-catchment, followed by area weighting for the whole sub-catchment. The classified LULC maps of 4 years and HSG maps were crossed to form different combinations/polygons, and the CN values were estimated for all the sub-catchments over the years 1990, 2000, 2010, and 2020. The CN values for type II category of antecedent moisture condition (AMC) were assigned to different combinations of four HSG classes and different categories of the LULC features following standard guidelines suggested in Singh et al. (1981).

Modeling runoff using HEC-HMS model

In this study, rainfall-runoff modeling is performed using the HEC-HMS model. A flowchart illustrating the step-by-step procedure for modeling streamflow and assessment of environmental flow is depicted in Fig. 2.

The HEC-HMS model considers different representations in the loss methods, transformation and baseflow separation techniques, and models in reach segments for simulation tasks (Zegelew and Langon 2020). This study considered soil conservation service (SCS)-curve number (CN) method and the SCS unit hydrograph method. The selection of these methods was dependent upon ease of applicability and less number of required data (Feldman 2000; Zegelew and Melese 2018). Theory and concepts of the methods are detailed in Feldman (2000) and USACE-HEC (2000).

The inputs such as rainfall, evaporation, soil type, and the hydrologic soil group were modeled into the HEC-HMS model. This study attempted at computing the environmental flow from the estimated runoff using rainfall data. Runoff was estimated based on the developed model under data-scarcity conditions where a comprehensive database of all the parameters was not available as the catchment was ungauged. Hence, a few of the information was considered based on the local understanding of the hydrological processes and from literature sources. The inputs such as canopy interception, surface depression storage, infiltration, precipitation conversion, etc., were estimated indirectly from the other inputs such as DEM, LULC, HSG, etc. The HEC-HMS has a component called soil moisture accounting (SMA) loss method. It has been used to model infiltration losses through methods used for computing initial abstractions losses such as surface

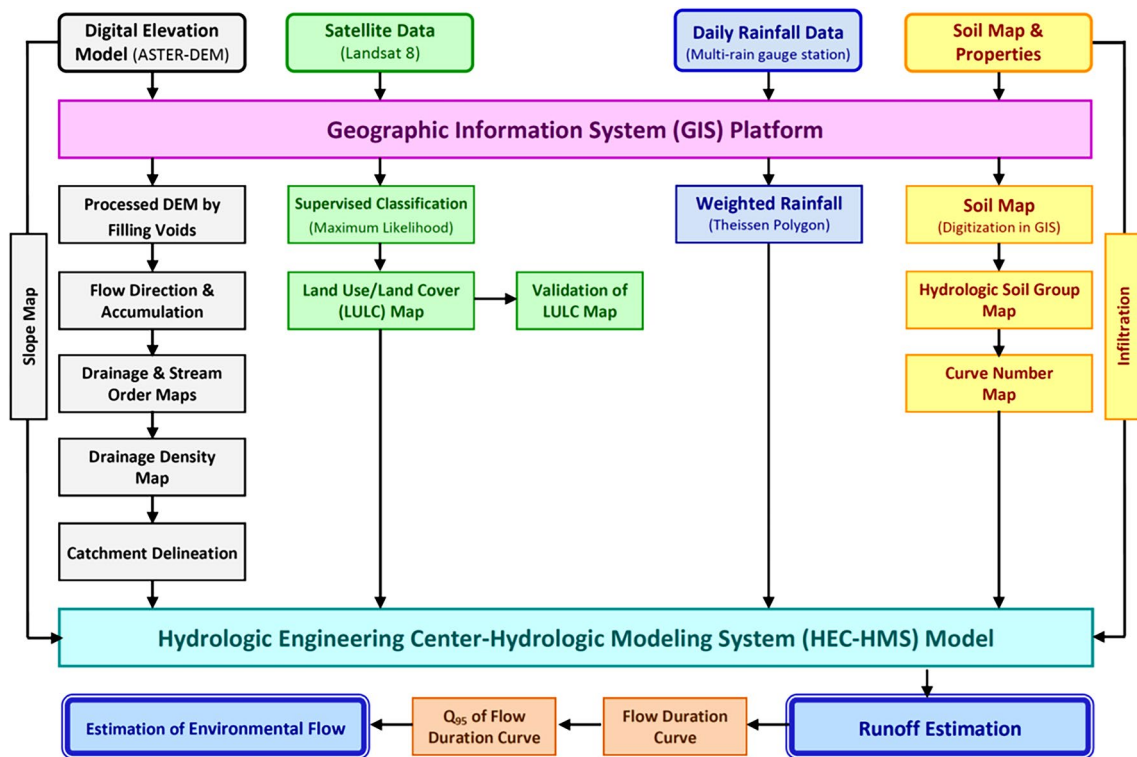


Fig. 2 Flowchart illustrating step-by-step methodology adopted for runoff estimation and environmental-flow estimation using geographic information system and HEC-HMS model

depression loss and canopy interception loss. The canopy represents the vegetation in the study area and is employed for continuous simulations. The excess rainfall flows as runoff (surface flow) after the canopy interception and the depression storage are filled. The infiltration rate triggers the runoff when it exceeds after fulfilling the canopy interception and depression storage losses. The maximum infiltration rate is the rate at which water flows from surface storage into the subsurface or sub-soil storage. The maximum infiltration rate is derived based on soil map of the catchment and representative values of saturated hydraulic conductivity. The value of the impervious area required in the model is computed from the urbanized area calculated from the developed LULC maps of the area. Soil water storage is defined as porosity, which is the available space that water can occupy in the soil. To model the runoff from the precipitation, the SCS unit hydrograph method was used. The time lag (T_{LAG}) (Eq. 1), an important concept in linear modeling of catchment response, was calculated using the following expression (Ouédraogo et al. 2018).

$$T_{LAG} = \frac{L \times 0.8 \times (S + 1) \times 0.7}{1900 \times \sqrt{Y}} \quad (1)$$

where T_{LAG} = lag time, L = hydraulic length of watershed, Y = percentage slope of watershed, and S = maximum retention in watershed.

$$S = \frac{25400}{CN - 254} \quad (2)$$

The CN was estimated for the sub-catchments (Eq. 2), based on the HSG and LULC maps representing four decades (1980–1990, 1991–2000, 2001–2010, and 2011–2018). After determining the required soil and LULC characteristics, the weighted CN values representing the four decades were estimated for each unit of the sub-catchment, followed by area-weighting for the whole sub-catchment.

Furthermore, for assuming the initial values of lag time (T_{LAG}) in the SCS unit hydrograph for each sub-catchment, transformation subroutine specifically designed for ungauged catchments (Scharffenberg and Fleming 2006) (Eq. 3) and a relation shown in Eq. (4) were also jointly applied.

$$t_c = 60 \times (11.9 \times L^3 |H|)^{0.385} \quad (3)$$

where L = length of the longest watercourse and H = elevation difference between divide and outlet (US-SCS 1986).

$$T_{lag} = 0.6 \times t_c \quad (4)$$

where t_c = time of concentration in minutes and T_{lag} = initial value of lag time.

In this study, linkages between rainfall and runoff were explored through empirical relationship and computing values of correlation coefficient (r) and coefficient of determination (R^2). These two evaluation criteria are summarized in Table 2.

Estimation of environmental flow

In this study, environmental flow was estimated for every month as well as for the year using their respective flow duration curves. The flow duration curve (FDC) is a chart representing the probability of exceedance on x -axis and runoff velocity or discharge on y -axis. The FDC method was selected for computing environmental flow in this study as this method is appropriately applicable even under the limited data-availability conditions due to deficiency of adequate quantum of runoff data or for a limited ability to focus on a significant environmental flow. In literature, the environmental flow or discharge value corresponding to 90 and 95% probability levels of exceedance (P_p) is termed as the minimal or environmental flow. However, looking at possibility of moderate runoff generation in the study catchment, 70 and 90% probabilities of exceedance are considered environmental flow in this study, which is computed using the Weibull’s plotting position formula as follows (Subramanya, 2013):

$$P_p = ((m|N + 1)) \times 100 \tag{5}$$

where N = no. of runoff or flow events and m = ranking of the runoff events.

Results and discussion

Slope and drainage network

Slope and drainage network maps of the study area are shown in Figs. 1 and 3, respectively. It is seen that slope

values are relatively less nearby water channels of drainage network. A total of 99.74 km² (15% of total area) lands mostly have 0–30% land slope. Lands under slope class of 30–60% contain 241.29 km² (35%) area and are mostly present far away from drainage channels. A major portion of the catchment, i.e., 340.05 km² (50%), have the steep slopes (> 60%), which is due to presence of hilly terrain in the area (Fig. 3). The steep-slope lands encompass a vast portion in the eastern part of study area where glacier exists. In general, the average land slope in the Himalayan region is more than 46% (Mahanta et al. 2016). Thus, the study catchment situated in Himalayan landscape, characterized by mountainous and hilly topography with steep slopes and limited soil depth constrained underlain by lithic rock, witness saturation-excess process of runoff generation (Needelman et al. 2004).

Drainage network map was used to characterize drainage pattern based on physical drainage characteristics such as joint angle, length of stream, and shortness. The drainage pattern helps understanding movement of runoff water over the catchment, as each pattern has different properties of conducting drainage. It is seen from Fig. 1 that a dendritic drainage pattern exists in the area, which is an indicator of favorable conditions for occurrence of groundwater potential due to its direct association with permeability and inverse relation with runoff (Machiwal et al. 2010).

Stream order

Stream order map (Fig. 4) shows that the study area comprises streams up to 5th order. It is observed that 1st-order streams constitute about 53.7% of total length of stream network followed by 19.5% length under 2nd-order streams, 8% length under 3rd-order streams, 10% length under 4th order, and 8.3% length under 5th-order streams. The higher is the order of the stream, the higher is the quantity of water drained. Here the low-order streams are relatively large in numbers, and hence, the water-yielding capacity of these streams usually remains high during rainy season. The low-order (2nd or 3rd order) streams are suitable for conserving runoff water by constructing

Table 2 Summary of two evaluation criteria

Evaluation criteria	Mathematical expression	Range of values			Reference
		Worst	Best	Acceptable	
Correlation coefficient (R)	$R = \left[\frac{\sum_{i=1}^N \{ (O_i - \bar{O}_i) (P_i - \bar{P}_i) \}}{\sqrt{\sum_{i=1}^N (O_i - \bar{O}_i)^2 \sum_{i=1}^N (P_i - \bar{P}_i)^2}} \right]^2$	0	1.0	0.5–1.0	Rodgers and Nicewander (1988); Machiwal and Jha (2014)
Coefficient of determination (R^2)	$R^2 = \frac{\sum_{i=1}^N \{ (O_i - \bar{O}_i) (P_i - \bar{P}_i) \}}{\sqrt{\sum_{i=1}^N (O_i - \bar{O}_i)^2 \sum_{i=1}^N (P_i - \bar{P}_i)^2}}$	0	1.0	0.5–1.0	Machiwal and Jha (2015)

Fig. 3 Percentage slope map of the study area

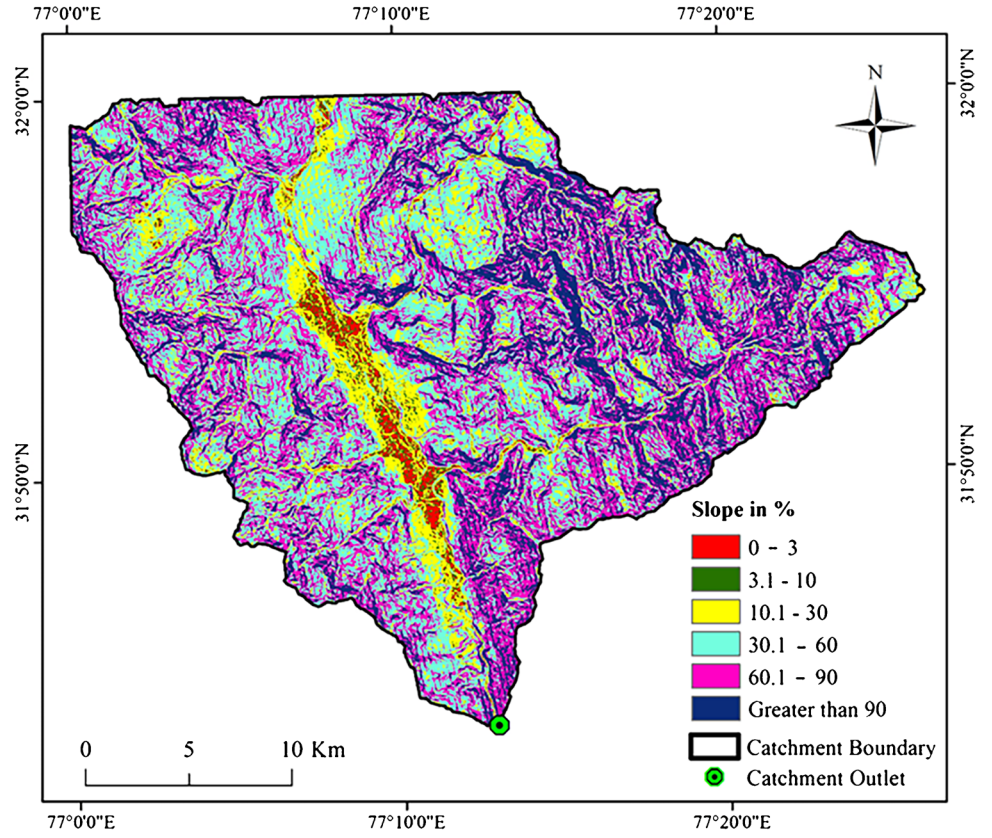
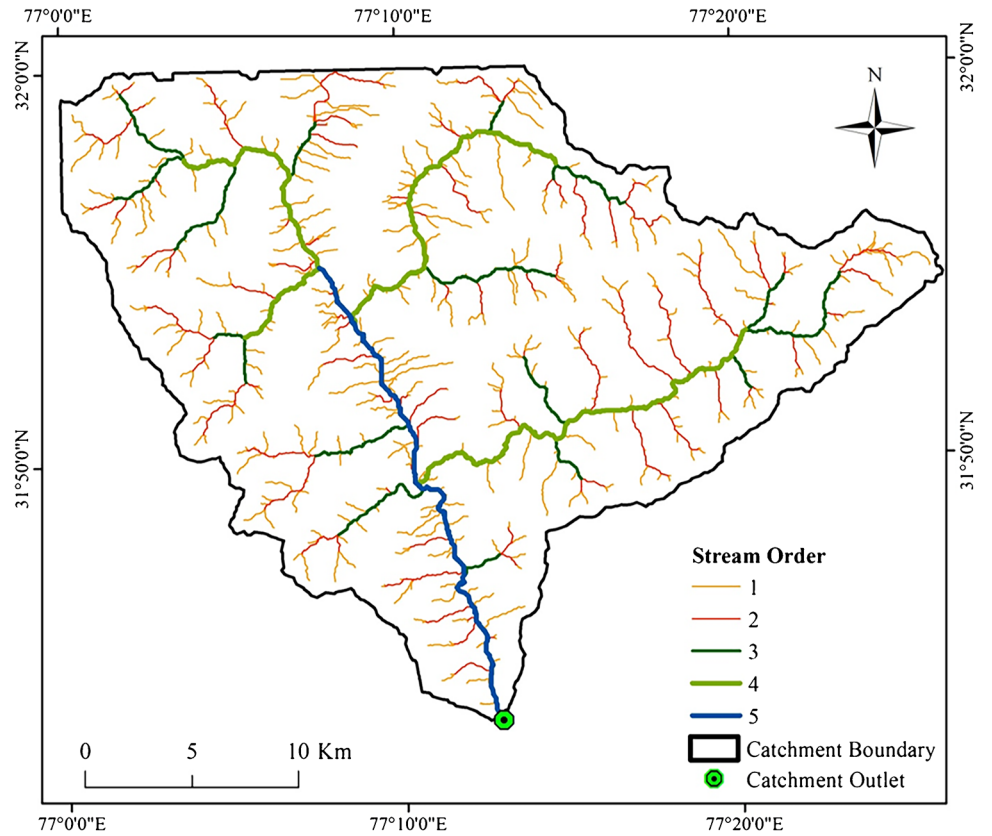


Fig. 4 Stream-order map of the study area



small structures such as check dams (Machiwal et al. 2010). Order-shrewd stream fragment’s total number is termed as stream number. The intensity of the infiltration and permeability depends upon the number of first-order streams (Hajam et al. 2013). On increasing an order of the stream, a few streams generally upsurge in geometric movement. In the study area, a total number of 1634 streams are present, of which 877 streams (54%) belong to the 1st-order streams that contributes the largest proportion to the overall drainage rate. This finding indicates that infiltration rate is quite high in the study area. A plot drawn between values of stream order versus values of stream number suggests that the drainage pattern is healthy in nature. Thus, it is inferred that good drainage conditions prevail in the catchment that contribute to the better water-holding capacity.

Drainage density

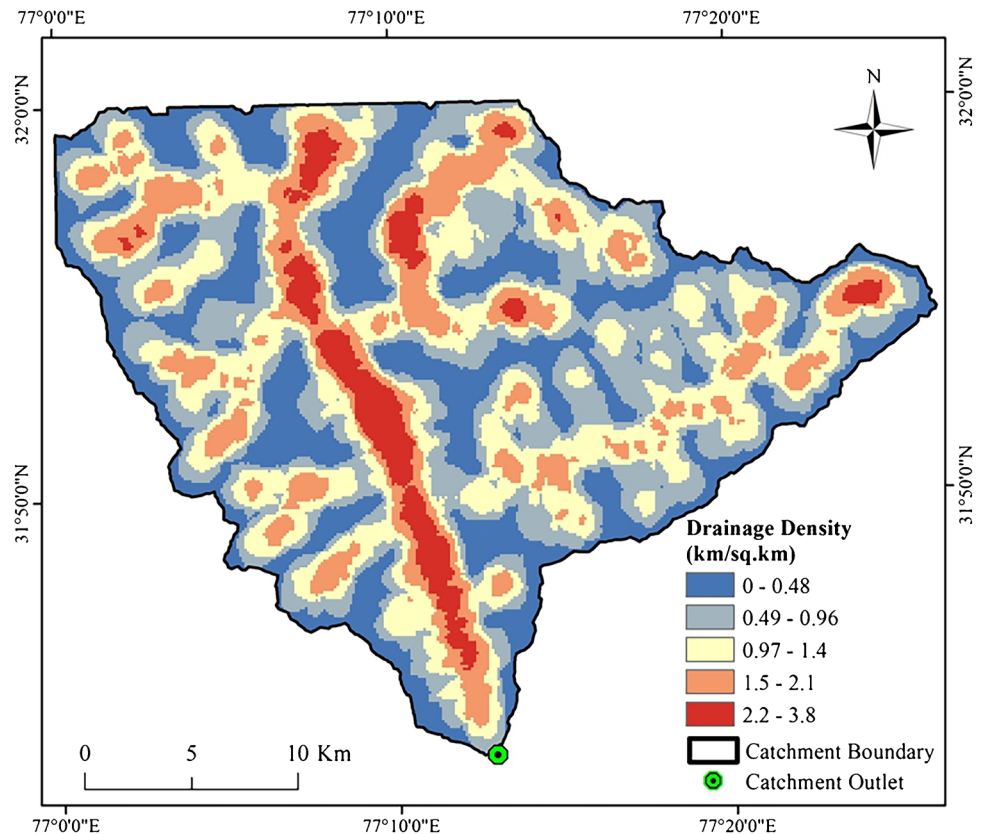
Drainage density map of the study area, classified into 5 classes, i.e., 0–0.48, 0.49–0.96, 0.97–1.4, 1.5–2.1, and 2.2–3.8 km km⁻², is shown in Fig. 5. It is seen that a major portion of the study area (367.88 km², 54% area) is covered with low values (< 0.95 km km⁻²) of drainage density (Fig. 5). On the other hand, drainage density is high (> 1.45 km km⁻²) in only 20% of the catchment area (139.53 km²)

where free-flow of water occurs following surface topology and the flowing water gets drained rapidly with less infiltration and less contribution to soil moisture and/or groundwater recharge resulting in poor vegetation (Machiwal et al. 2015). In contrast, areas having low drainage density are likely to have a high vegetation cover in the area due to less runoff generation and adequate soil moisture in subsurface layers (Kumar et al. 2019).

Variability of monthly and annual rainfall

Bar charts of the mean monthly rainfall for three rain gauge stations are shown in Fig. 6(a) along with standard deviation values shown as error bars. It is seen that monthly rainfall is relatively high in four monsoon months, i.e., June through September, which have the maximum mean contribution, of 42, 70, and 78% to annual rainfall of Bhuntar, Sundernagar, and Dharamsala stations. Standard deviation of rainfall is high in monsoon months when the mean rainfall remains high. At Bhuntar station, value of coefficient of variation (CV) remains the lowest (51 to 56%) in the months of February, March, July, and August when the mean monthly rainfall is more than 100 mm. At Sundernagar, the lowest CV values (35 to 58%) are observed in monsoon months having the mean rainfall varying from 131 to 354 mm. Similar to the other two stations, the CV values at Dharamsala station are

Fig. 5 Drainage density map of the study area



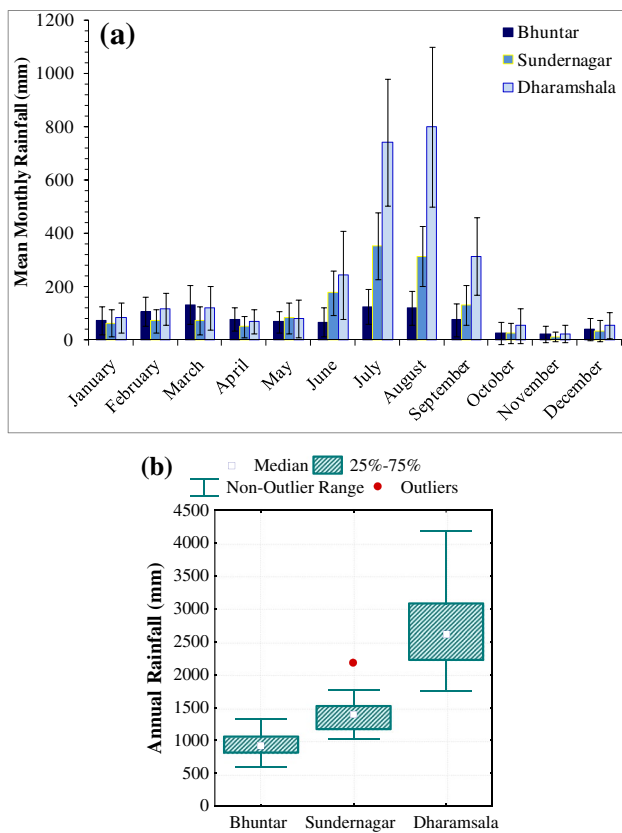


Fig. 6 **a** Bar charts of the mean monthly rainfall along with error bars showing standard deviation and **b** box-whisker plots of annual rainfall for three stations

the lowest (32 to 47%) during July, August, and September when the mean rainfall ranges from 314 to 801 mm. Skewness values in monthly rainfall series are positive for all the stations, indicating a right-skewed rainfall distribution. Kurtosis values varied from (–)1.02 to 7.29 for Bhuntar, (–)0.80 to 3.83 for Sundernagar, and (–)0.57 to 5.53 for Dharamshala. Positive (negative) kurtosis values indicate a heavy-tailed (light-tailed) distribution of the rainfall data with a sharper (flatter) peak in comparison to the normal distribution curve.

The mean annual rainfalls for Bhuntar, Sundernagar, and Dharamshala stations are 930 ± 180 , 1387 ± 237 , and 2704 ± 587 mm, respectively, with corresponding CV values of 19, 17, and 22%. Almost similar rainfall variability in terms of CV values was reported in a previous study for three stations of Kullu valley, i.e., 18.5% for Kullu valley 21.7% for Bajaura, and 24.2% for Katrain (Jangra and Singh 2011). Overall, the mean annual rainfall of the area is 1377 mm, ranging from the monthly minimum rainfall of 63 mm (January) to the monthly maximum rainfall of 344 mm (July). Box-whisker plots of 39-year annual rainfall for three stations are shown in Fig. 6(b). A big difference in the median rainfall of three stations is apparent, which suggests large rainfall variability in the area. Annual rainfall of Bhuntar

is uniform as lengths of the upper and lower whiskers are almost equal, whereas the presence of one outlier at Sundernagar and relatively large length of the upper whisker at Dharamshala indicate presence of the right skewness in the rainfall, which confirms the earlier finding based on the positive values of skewness.

Land use/land cover maps

Collection of ground truth data for quantitative assessment of accuracy of the developed LULC map could not be possible in this study mainly due to presence of mountainous terrain (Morley et al. 2018) and also for the reason that some part of lands was inaccessible. Hence, the developed land use/land cover (LULC) map of the study catchment were verified through visual comparison with toposheets and Google Earth image along with visiting some sites for their confirmation. Hence, accuracy assessment of the LULC map may be quantitatively accomplished in future studies subject to availability of ground truth data. It is seen that the study area mainly contains six types of LULC classes, i.e., agricultural land, barren land, water bodies, glacier, built-up land, and forest land (Fig. 7a–d). In the study area, a large amount of soil loss occurs that has a significant impact on land use changes especially interactions among forest lands, barren lands, and glacier. In recent times, it is seen from LULC map of 2020 that forests having a spread of 418.56 km^2 lands (61.4% of study area) is the dominating LULC type all over the study area. Barren land exists in 114.64 km^2 (16.8%) area mainly located in western and northern portions of the area. Agricultural land encompasses 102.61 km^2 (15%) lands mostly in a north-south stretch that is close to the drainage network (rivers and streams). Three LULC classes (glacier, water bodies, and built-up land) cover only 45.32 km^2 (6.65%) of the area. The resultant LULC maps (Fig. 7) have been validated with the SOI topographical maps and the Google earth images.

Hydrologic soil group and curve number

Soil map of the study area was categorized into four hydrologic soil groups (HSG) that are A, B, C, and D based on infiltration potential and runoff generating capacity. The classified HSG map is illustrated in Fig. 8. It is seen that class A of HSG having the highest infiltration and less runoff generating potential is not present in the study area. A major portion of the study area is covered by class C (477.94 km^2 , 66%) of HSG type, followed by class B (225.75 km^2 , 31%), class A (8.35 km^2 , 0.1%), and class D (4.27 km^2 , 0.06%). It is apparent that class C–type HSG mostly exists in nearby drainage lines in the area where lands are used for agriculture. Class D of HSG is located over a small patch on eastern part of the area representing

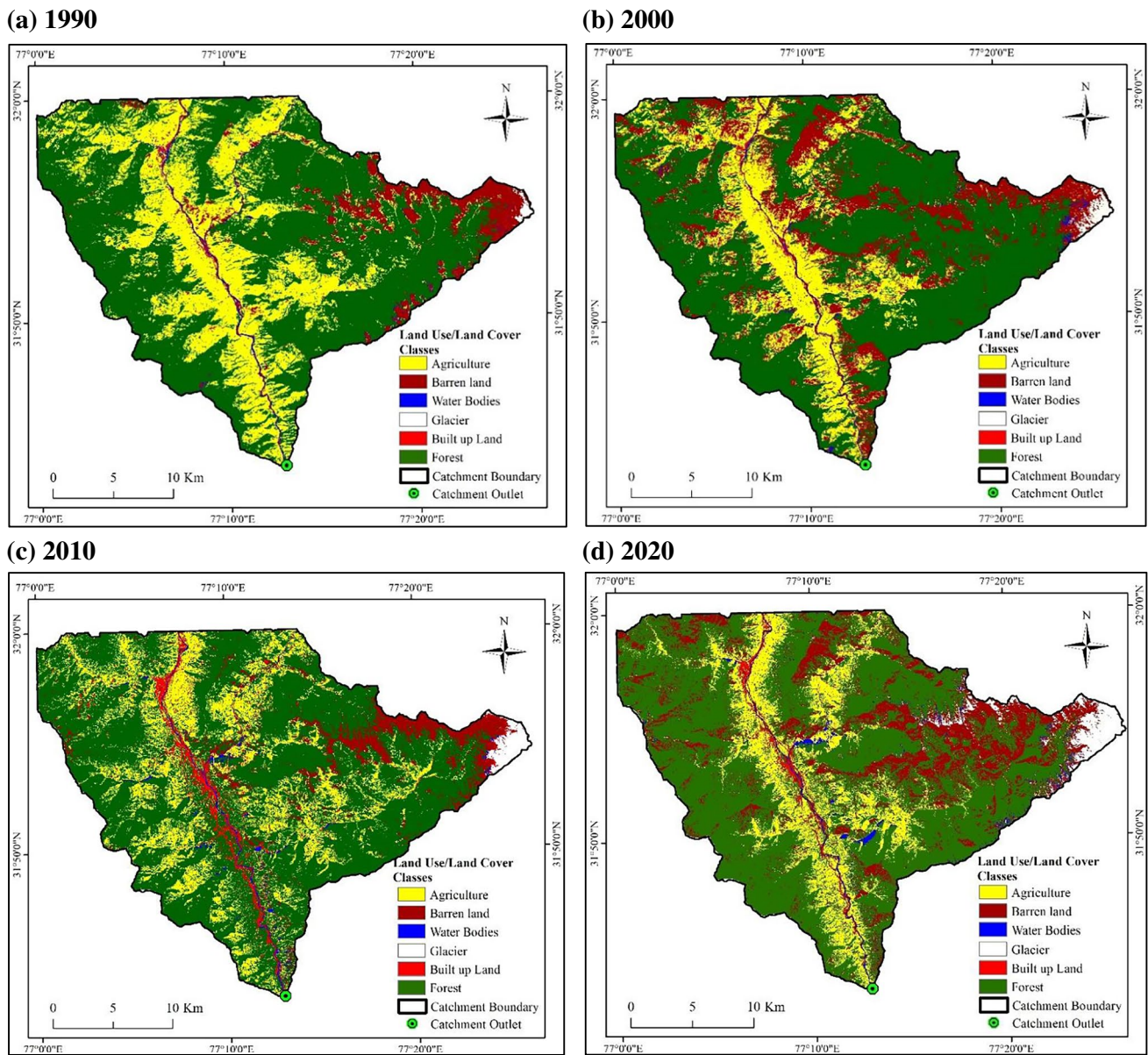
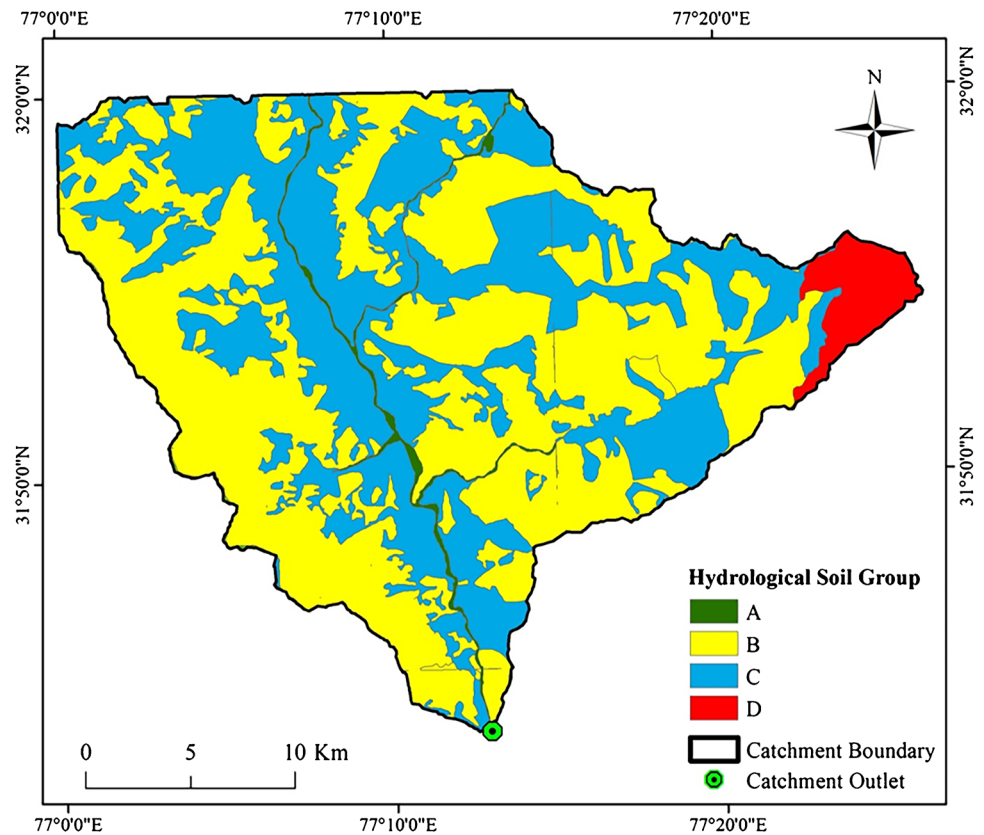


Fig. 7 Land use/land cover maps of the study area for years **a** 1990, **b** 2000, **c** 2010, and **d** 2020

glacier. Overall, the HSG map shows that the runoff generation should be moderate in this region (Rao 2020); however, runoff is also controlled by slope, drainage network, and stream orders.

The Landsat satellite data were used to abstract and incorporate four maps of spatially distributed LULC representing four decades for computation of the CN values. The Soil Conservation Service-Curve Number (SCS-CN) table provides values of CN for different combinations of LULC and HSG. Values for the initial abstraction losses, i.e., canopy (vegetation) interception and surface/depression storage (Tables 3 and 4), were obtained from the analysis of LULC and DEM, respectively. The total area under the

canopy/vegetation was calculated from the LULC map and was given as the value of initial storage or loss (in %). Thereafter, the maximum water storage (in mm) was derived based on the percentage of the total land area under vegetation (Table 3). Similarly, for computing depression storage, the calculated slope values were classified into different ranges and percentage land area contributing to the flat slope (0–5%) was derived for the sub-basins. The corresponding maximum storage values (in mm) are taken from Table 4. The values of canopy interception and depression storage presented in Tables 3 and 4 are considered the standards, which are derived based on the experiments carried out earlier for different vegetation types and topographic slopes.

Fig. 8 Hydrological soil group map of the study area**Table 3** Canopy/vegetation interception values (source: Holberg 2014)

Type of vegetation	Canopy interception (mm)
General vegetation	1.270
Grasses and deciduous trees	2.032
Coniferous trees	2.540

Table 4 Surface depression storage values (source: Ouédraogo et al. 2018)

Description	Slope (%)	Surface storage (mm)
Paved impervious areas	-	3.18–6.35
Flat, furrowed land	0–5	50.8
Moderate to gentle slopes	5–30	6.35–12.70
Steep, smooth slopes	> 30	1.02

The flat slopes have the maximum surface storage capacities. Finally, canopy interception loss as well as surface depression loss was subtracted from the total runoff generated in the catchment as estimated from the SCS-CN method. The CN values for each map unit were aggregated for the whole catchment by means of GIS to obtain a weighted CN value.

Computation of the weighted CN value for the year 2020 is illustrated in Table 5. It is seen that the CN values for different map polygons varied from 55 to 100 (Table 5), which are in close harmony to that reported in the literature, ranging from 69 to 100, for the study area (Singh et al. 2021). The computed values of the weighted CN for the years 1990, 2000, 2010, and 2020 were found to be 70.51, 70.36, 70.16, and 70.54, respectively, in this study.

Rainfall-runoff relationship

Daily runoff values estimated by the HEC-HMS model for the period 1980–2018 were plotted over time scale and the same is shown in Fig. 9. Large fluctuations in daily runoff values along with cyclic patterns are apparent, which are due to seasonal nature of the annual rainfall that is mostly concentrated over the monsoon months of June through September. It is further seen that the runoff values had an increasing trend over the period 1980–1995 and decreasing trends from 1995 to 2008 and from 2011 to 2017. The peak runoff rate in the area exceeded the value of $2000 \text{ m}^3 \text{ s}^{-1}$ four times with an abrupt shift/change in the runoff values in years 1992, 1998, and 2018. Validation of the model-estimated runoff, as done in most of the past rainfall-runoff studies, could not be possible in this study due to non-availability of observed runoff data as the catchment is ungauged. However, in order

Table 5 Computation of curve number values for the year 2020

Land use/land cover	Soil texture	Area (km ²)	Area (%)	Hydrologic soil group	Curve number	(%Area × CN)/100	Weighted curve number
Agriculture	Coarse	41.849	6.14	B	75	4.61	70.54
	Fine	60.7599	8.92	C	85	7.58	
Forest	Coarse	251.5173	36.93	B	55	20.31	18.88
	Fine	167.0383	24.52	C	77	18.88	
Barren land	Coarse	53.12411	7.80	B	69	5.38	7.59
	Fine	61.52129	9.03	C	84	7.59	
Water bodies	Coarse	10.3293	1.52	A	100	1.52	
Glacier	Coarse	17.0703	2.51	D	100	2.51	
Built up land	Coarse	3.405648	0.50	B	70	0.35	1.81
	Fine	14.50985	2.13	C	85	1.81	

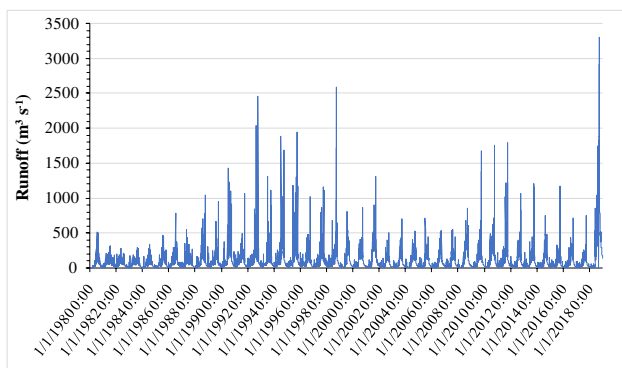
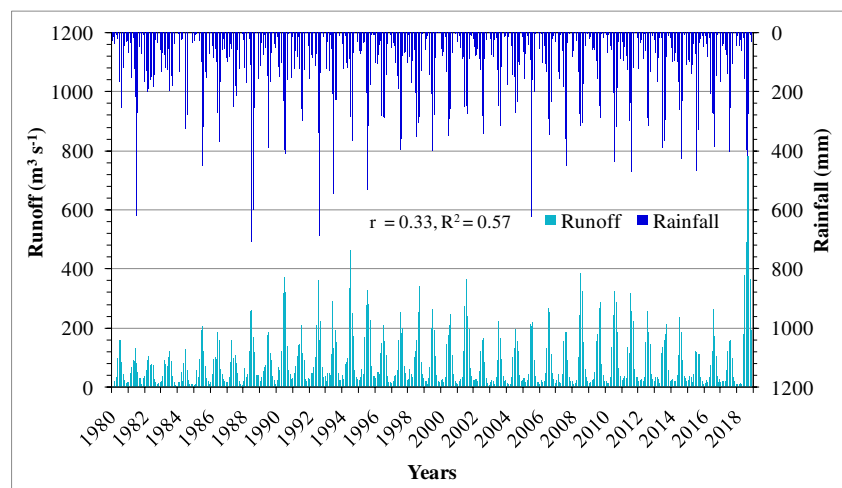


Fig. 9 Time plot of daily runoff estimated using HEC-HMS model for the period 1980–2018

to understand effect of rainfall on runoff, bar charts of both the variables were plotted at monthly time scale, and the same is shown in Fig. 10. A visual comparison of bar charts of rainfall and runoff showed that the peaks and troughs

Fig. 10 Bar charts of monthly rainfall and runoff values over 39-year period (1980–2018)



of the runoff bars did not exactly correspond to that of the rainfall bars. Also, the proportion of rainfall to runoff rate did not remain the constant over 39-year period, which may be due to considering rate of runoff in this study, instead the total quantity of monthly runoff that might depict a direct relationship with rainfall. Besides, there may be other reasons such as rainfall intensity, time of concentration, and antecedent moisture conditions for the infirm rainfall-runoff relationship. Furthermore, in this study, there are a few other factors also, i.e., snowmelt runoff, environmental flow, dense forest vegetation, and mountainous terrain, that could be the possible reasons for the slight mismatch in the rainfall and runoff.

Mathematical or statistical techniques are always recommended to be adopted in addition to graphical tools in hydrological studies (Machiwal and Jha 2008). Hence, linear regression was employed in this study to determine statistical significance of the relationship between rainfall and runoff over 39-year period. The results of regression revealed values of goodness-of-fit criteria, i.e., r and R^2 as 0.57 and

0.33, respectively, which revealed a moderate to weak positive relationship between rainfall and runoff. The poor rainfall-runoff relationship may also be due to incapability of the empirical model in generating actual runoff values as the model could not be calibrated under non-availability of observed runoff data for the ungauged catchment. Similar weak to moderate correlations between rainfall and runoff were reported in earlier studies performed in Himalayan catchment of Nepal ($r \sim 0.37\text{--}0.82$) (Merz et al. 2006) and India ($R^2 \sim 0.43\text{--}0.81$) (Qazi 2020). Likewise, regression-based rainfall-runoff modeling in Wadi Ahim catchment of Oman revealed a relationship between rainfall and runoff with R^2 -value of 0.60 (McIntyre et al. 2007).

The poor rainfall-runoff relationships have also been reported in earlier studies performed in ungauged catchments especially in the hilly terrain due to some limitations experienced in hydrological modeling that results in less accurate runoff predictions. The hydrologic models employing regional relationship between hydrologic response characteristics and landscape attributes have successfully predicted runoff in an ungauged catchment (Post and Jakeman 1999). However, hydrographs developed from the results were poor in some cases mainly because of poor understanding of the relationships between hydrologic response and physical attributes. In fact, precise estimation of runoff in an ungauged catchment poses a serious challenge to hydrologists (Wagener and Wheater 2006), which is overcome to some extent through parameter regionalization processes, i.e., spatial proximity, regression modeling, and physical similarity (Petheram et al. 2012; Zhang et al. 2015; Kim 2016). Furthermore, contribution of snowmelt water to runoff is somewhat difficult to model and account in the hydrological models, and this may be considered one of the major limitations in rainfall-runoff modeling (De Scally 1994; Archer and Fowler 2008; Pool et al. 2017; Akanegbu et al. 2018). In another study carried out in ungauged catchment of Australia, Boughton and Chiew (2007) emphasized selection of rainfall data to represent the runoff-generating rainfall over the catchment for the better runoff predictions. In addition, there may be other possible reasons for poor rainfall-runoff modeling, which include inadequate representation of spatial and temporal rainfall variabilities over the catchment (Hughes 1995) and inadequate estimation of parameter values (Görgens 1983).

Environmental flow

The FDCs were plotted for 12 months and annually representing runoff values estimated by the HEC-HMS model at different probabilities of exceedance ranging from 0 to 100th percentiles for the study catchment. The FDC drawn for the annual runoff over 39-year period is presented in Fig. 11. It is seen that environmental flow values declined drastically

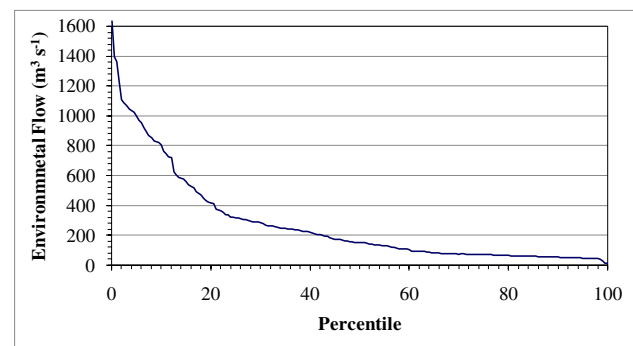


Fig. 11 Flow duration curve for the period 1980–2018

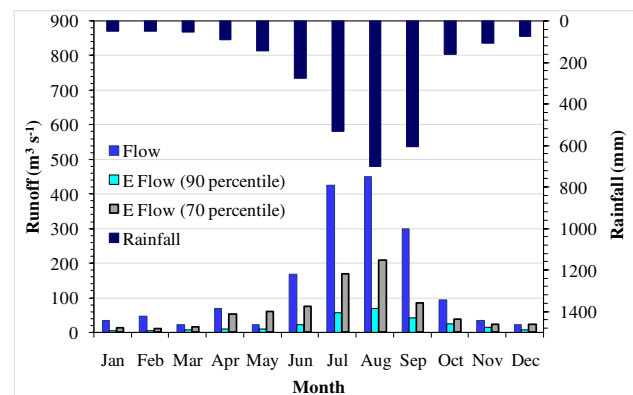


Fig. 12 Bar charts of monthly average rainfall, runoff, and environmental flow

from the highest at 0 percentile to 20th percentile. Afterward, the rate of declination of the FDC decreased until the 99th percentile value of probability of exceedance. It is seen that value of the FDC at 70th percentile (Q_{70}) and 90th percentile (Q_{90}) corresponded to 75 and 55 $\text{m}^3 \text{s}^{-1}$, respectively, which represents the annual environmental flow. The annual environmental flow should always be maintained in the dam every year to sustain the living beings that are dependent upon the river flow.

The mean values of the monthly environmental flow computed from the monthly FDCs along with the mean monthly rainfall and runoff for 39-year period are shown through bar charts in Fig. 12. It is seen that both the mean monthly runoff and environmental flow are in harmony with the mean monthly rainfall. Also, the peak of runoff value ($450.82 \text{ m}^3 \text{ s}^{-1}$) as well as peak of environmental flow ($207.68 \text{ m}^3 \text{ s}^{-1}$ at 70th percentile and $67.65 \text{ m}^3 \text{ s}^{-1}$ at 90th percentile) appeared in August month, which corresponded well with that of rainfall (699 mm) of August month. This finding, emphasizing a fair relationship among rainfall, runoff, and environmental flow, further verified the competence of the HEC-HMS model in estimating the monthly runoff and environmental flow satisfactorily. Unavailability of observed runoff data

due to ungauged catchment in this study was the major limitation of this study; however, the model-estimated runoff as well as computed environmental flow was reasonably linked to observed rainfall patterns in order to justify the potency of the rainfall-runoff modeling performed. Moreover, the approach adopted in this study to test the model adequacy and verify the model outcomes may be suitably adopted for other ungauged catchments in different parts of the world.

Conclusions

This study performed rainfall-runoff modeling using the conceptual HEC-HMS model in a Himalayan catchment of India where estimates of surface runoff and environmental flow are of prime importance to alleviate environmental impacts of hydropower project. Conceptual modeling aimed to reproduce the hydrological behavior of a catchment during a rainy event. The drainage pattern was delineated using ArcGIS and modeled according to the reaches, sub-catchment, etc. The curve number was derived from the land use/land cover and hydrologic soil group and it was fed into the model. The collected precipitation data were fed on the hourly basis for each sub-catchment based on their concentration in the region.

The slope was more than 60% in half of the catchment, suggesting high slope steepness with dendritic drainage pattern as the terrain was mountainous. About 1634 number of streams was present in the catchment and more than 54% of them were of 1st order having high infiltration rate and the highest contribution to the catchment's drainage rate. Drainage density values in more than half of the catchment were less than 0.95 km km^{-2} , which indicated moderate potential for runoff generation and high vegetation cover. Annual rainfall in the study area depicted a high variability over space with positive skewness over years. Land use/land cover map of the study area revealed that forest lands occupying 423.83 km^2 area encompass 62% of the study area. Likewise, about 477.94 km^2 lands were covered with class C of hydrologic soil group, which suggested moderate runoff generation potential in the catchment. Crossing of land use/land cover and hydrologic soil group maps in geographic information system revealed a weighted average value of curve number as 69.23, which further indicated a relatively moderate potential of runoff generation in the catchment. A gradual trend was seen in the estimated runoff that was inclining during 1980–1995 and declining during 1995–2008 and 2011–2017. Besides, an abrupt change in runoff was observed in years 1992, 1998, and 2018 when the peak rate of runoff exceeded more than $2000 \text{ m}^3 \text{ s}^{-1}$. The model outcomes could not depict a perfect coherence between peaks and troughs of runoff and rainfall values in a bar chart. Further, rainfall did not contribute constantly to

runoff every year due to influence of other factors on runoff generation. Reasonable moderate-to-weak relationship was observed between rainfall and runoff from values of two goodness-of-fit criteria, i.e., r (0.57) and R^2 (0.33). The annual value of environmental flow was obtained as 75 and $55 \text{ m}^3 \text{ s}^{-1}$ at 70th and 90th percentiles, respectively, from the flow duration curve. In addition, the mean monthly peak values of runoff and environmental flow at 70th and 90th percentiles were obtained as 450.82, 207.68, and $67.65 \text{ m}^3 \text{ s}^{-1}$, respectively, in August month, which were in harmony. Overall, the approach and findings of this study are useful for runoff potential in other ungauged catchments under limited data-availability conditions.

Acknowledgements The authors are grateful to the two anonymous reviewers for their valuable comments, which improved quality of an early version of this manuscript.

Funding The funds received from DOES&T, Himachal Pradesh, India, to carry out this study are gratefully acknowledged.

Data Availability Data will be made available on a reasonable request.

Declarations

Conflict of interests The authors declare that they have no competing interests.

References

- Akanegbu JO, Meriö LJ, Marttila H, Ronkanen AK, Kløve B (2018) A simple model structure enhances parameter identification and improves runoff prediction in ungauged high-latitude catchments. *J Hydrol* 563:395–410
- Akinwumi AM, Adewumi JR, Obiora-Okeke OA (2021) Impact of climate change on the stream-flow of Ala River, Akure, Nigeria. *Sustain Water Resour Manag* 7:1. <https://doi.org/10.1007/s40899-020-00484-7>
- Anandharuban P, Rocca ML, Elango L (2019) A box-model approach for reservoir operation during extreme rainfall events: a case study. *J Earth Syst Sci* 128:229. <https://doi.org/10.1007/s12040-019-1258-7>
- Archer D, Fowler H (2008) Using meteorological data to forecast seasonal runoff on the River Jhelum, Pakistan. *J Hydrol* 361:10–23
- Azmat M, Choi M, Kim TW, Liaqat UW (2016) Hydrological modeling to simulate streamflow under changing climate in a scarcely gauged cryosphere catchment. *Environ Earth Sci* 75:186. <https://doi.org/10.1007/s12665-015-5059-2>
- Azmat M, Qamar MU, Ahmed S, Hussain E, Umair M (2017) Application of HEC-HMS for the event and continuous simulation in high altitude scarcely-gauged catchment under changing climate. *Eur Water* 57:77–84
- Boughton W, Chiew F (2007) Estimating runoff in ungauged catchments from rainfall, PET and the AWBM model. *Environ Model Softw* 22(4):476–487
- De Scally FA (1994) Relative importance of snow accumulation and monsoon rainfall data for estimating annual runoff, Jhelum basin, Pakistan. *Hydrol Sci J* 39:199–216

- Ditthakhit P, Pinthong S, Salaeh N, Binnui F, Khwanchum L, Pham QB (2021) Using machine learning methods for supporting GR2M model in runoff estimation in an ungauged basin. *Sci Rep* 11:19955. <https://doi.org/10.1038/s41598-021-99164-5>
- Görgens AHM (1983) Reliability of calibration of a monthly rainfall-runoff model: the semiarid case. *Hydrol Sci J* 28(4):485–498
- Guo H, Chen S, Bao A, Hu J, Gebregiorgis A, Xue X, Zhang X (2015) Inter-comparison of high-resolution satellite precipitation products over central Asia. *Remote Sens* 7:7181–7211
- Gyawali, R. and Watkins, D.W. (2013). Continuous hydrologic modeling of snow-affected watersheds in the Great Lakes basin using HEC-HMS. *Journal of Hydrologic Engineering, ASCE*, 18: 29-39
- Haan CT (2002) *Statistical Methods in Hydrology* (2nd edition). Iowa State Press, Ames, p 496
- Hajam RA, Hamid A, Bhat S (2013) Application of morphometric analysis for geo-hydrological studies using geo-spatial technology—a case study of Vishav Drainage Basin. *Hydrol Curr Res* 4(3):1–12
- Holberg J (2014) Tutorial on Using HEC-GeoHMS to develop soil moisture accounting method inputs for HEC-HMS. Purdue University, West Lafayette, IN, USA
- Hughes DA (1995) Monthly rainfall-runoff models applied to arid and semiarid catchments for water resource estimation purposes. *Hydrol Sci J* 40(6):751–769
- Hunukumbura PB, Weerakoon SB, Herath S (2008) Runoff modeling in the upper Kotmale Basin. In: Hennayake N, Rekha N, Nawfal M, Alagan R, Daskon C (eds) *Traversing no man's land, interdisciplinary essays in honor of Professor Madduma Bandara*. University of Peradeniya, Sri Lanka, pp 169–184
- Jangra S, Singh M (2011) Analysis of rainfall and temperatures for climatic trend in Kullu valley. *MAUSAM* 62(1):77–84
- Joo J, Thomas K, Kim H, Lee H (2014) A comparison of two event-based flood models (ReFH-rainfall runoff model and HEC-HMS) at two Korean catchments, Bukil and Jeungpyeong. *KSCE J Civ Eng* 18(1):330–343
- Khatri HB, Jain MK, Jain SK (2018) Modelling of streamflow in snow dominated Budhigandaki catchment in Nepal. *J Earth Syst Sci* 127:100. <https://doi.org/10.1007/s12040-018-1005-5>
- Kim HS (2016) Potential improvement of the parameter identifiability in ungauged catchments. *Water Resour Manag* 30:3207–3228
- Kumar D, Bhattacharjya RK (2020) Evaluating two GIS-based semi-distributed hydrological models in the Bhagirathi-Alkhnanda River catchment in India. *Water Policy* 22:991–1014
- Kumar S, Machiwal D, Parmar BS (2019) Parsimonious approach to delineate groundwater potential zones using geospatial modeling and MCDA techniques under limited data availability condition. *Eng Rep*. <https://doi.org/10.1002/eng2.12073>
- Leimer S, Pohlert T, Pfahl S, Wilcke W (2011) Towards a new generation of high-resolution meteorological input data for small scale hydrological modeling. *J Hydrol* 402(3–4):317–332
- Machiwal D, Jha MK (2008) Comparative evaluation of statistical tests for time series analysis: application to hydrological time series. *Hydrol Sci J* 53(2):353–366
- Machiwal, D. and Jha, M.K. (2012). *Hydrologic time series analysis: theory and practice*. Springer, the Netherlands and Capital Publishing Company, New Delhi, India, pp. 303
- Machiwal D, Jha MK (2014) Characterizing rainfall-groundwater dynamics in a hard-rock aquifer system using time series, GIS and geostatistical modeling. *Hydrol Process* 28(5):2824–2843
- Machiwal D, Jha MK (2015) GIS-based water balance modeling for estimating regional specific yield and distributed recharge in data-scarce hard-rock region. *J Hydro-environ Res* 9(4):554–568
- Machiwal D, Kumar S, Islam A, Kumar S, Jat SR, Vaishnav M, Dayal D (2021) Evaluating effect of cover crops on runoff, soil loss and soil nutrients in an Indian arid region. *Commun Soil Sci Plant Anal* 52(14):1669–1688
- Machiwal D, Rangi N, Sharma A (2015) Integrated knowledge- and data-driven approaches for groundwater potential zoning using GIS and multi-criteria decision making techniques on hard-rock terrain of Ahar catchment, Rajasthan, India. *Environ Earth Sci* 73(4):1871–1892
- Machiwal D, Srivastava SK, Jain S (2010) Estimation of sediment yield and selection of suitable sites for soil conservation measures in Ahar River basin of Udaipur, Rajasthan using RS and GIS techniques. *J Indian Soc Remote Sens* 38(4):696–707
- Mahanta B, Singh HO, Singh PK, Kainthola A, Singh TN (2016) Stability analysis of potential failure zones along NH-305, India. *Nat Haz* 83:1341–1357
- Makungo R, Odiyo JO, Ndiritu JG, Mwaka B (2010) Rainfall-runoff modelling approach for ungauged catchments: a case study of Nzhelele River sub-quaternary catchment. *Phys Chem Earth* 35:596–607
- McIntyre N, Al-Qurashi A, Wheeler H (2007) Regression analysis of rainfall-runoff data from an arid catchment in Oman. *Hydrol Sci J* 52(6):1103–1118
- Merz J, Dangel PM, Dhakal MP, Dongol BS, Nakarmi G, Weingartner R (2006) Rainfall-runoff events in a middle mountain catchment of Nepal. *J Hydrol* 331:446–458
- Morley PJ, Donoghue DNM, Chen J-C, Jump AS (2018) Integrating remote sensing and demography for more efficient and effective assessment of changing mountain forest distribution. *Ecol Inform* 43:106–115
- Natarajan S, Radhakrishnan N (2021) Simulation of rainfall-runoff process for an ungauged catchment using an event-based hydrologic model: a case study of Koraiyar basin in Tiruchirappalli city, India. *J Earth Syst Sci* 130:30. <https://doi.org/10.1007/s12040-020-01532-8>
- Needelman BA, Gburek WJ, Petersen GW, Sharpley AN, Kleinman PJA (2004) Surface runoff along two agricultural hillslopes with contrasting soils. *Soil Sci Soc Am J* 68:914–923
- Ouédraogo WAA, Raude JM, Gathenya JM (2018) Continuous modeling of the Mkurumudzi River catchment in Kenya using the HEC-HMS conceptual model: calibration, validation, model performance evaluation and sensitivity analysis. *Hydrology* 5(3):44. <https://doi.org/10.3390/hydrology5030044>
- Petheram C, Rustomji P, Chiew FHS, Vleeshouwer J (2012) Rainfall-runoff modelling in northern Australia: a guide to modelling strategies in the tropics. *J Hydrol* 462:28–41
- Pokhrel BK, Chevallier P, Andréassian V, Tahir AA, Arnaud Y, Neppel L, Budhathoki KP (2014) Comparison of two snowmelt modeling approaches in the DudhKoshi basin (eastern Himalayas, Nepal). *Hydrol Sci J* 59(8):1507–1518
- Pool S, Viviroli D, Seibert J (2017) Prediction of hydrographs and flow-duration curves in almost ungauged catchments: which runoff measurements are most informative for model calibration? *J Hydrol* 554:613–622
- Post DA, Jakeman AJ (1999) Predicting the daily streamflow of ungauged catchments in SE Australia by regionalising the parameters of a lumped conceptual rainfall-runoff model. *Ecol Model* 123(2–3):91–104
- Feldman (2000) *Hydrologic modeling system HEC- HMS: technical reference manual*. CPD-74B. US Army Corps of Engineers. Hydrologic Engineering Center, Davis, California, pp 145
- Prasad AS, Pandey BW, Leimgruber W, Kunwar RM (2016) Mountain hazard susceptibility and livelihood security in the upper catchment area of the river Beas, Kullu Valley, Himachal Pradesh, India. *Geoenviro Disasters* 3(1):1–17
- Qazi N (2020) Hydrological functioning of forested catchments, Central Himalayan Region, India. *For Ecosyst* 7:63. <https://doi.org/10.1186/s40663-020-00275-8>

- Rao KN (2020) Analysis of surface runoff potential in ungauged basin using basin parameters and SCS-CN method. *Appl Water Sci* 10:47. <https://doi.org/10.1007/s13201-019-1129-z>
- Rezaeianzadeh M, Stein A, Tabari H, Abghari H, Jalalkamali N, Hosseinipour E, Singh VP (2013) Assessment of a conceptual hydrological model and artificial neural networks for daily outflows forecasting. *Int J Environ Sci Technol* 10:1181–1192
- Rodgers JL, Nicewander WA (1988) Thirteen ways to look at the correlation coefficient. *The American Statistician* 42(1):59–66
- Scharffenberg, W.A. and Fleming, M.J. (2006). Hydrologic modeling system HEC-HMS: User's manual. United States Army Corps of Engineers, Hydrologic Engineering Center.
- Seibert J (1999) Regionalisation of parameters for a conceptual rainfall-runoff model. *Agr For Meteorol* 98:279–293
- Sharma P, Machiwal D (2021) Streamflow forecasting: overview of advances in data-driven techniques. In: Sharma P, Machiwal D (eds) *Advances in streamflow forecasting – from traditional to modern approaches*. Elsevier, Netherlands, pp 1–48
- Singh, G., Venkataramanan, C., and Sastry, G. (1981). *Manual of soil and water conservation practices in India*. Central Soil and Water Conservation Research and Training Institute, Dehradun, India, pp. 434.
- Singh S, Dhote PR, Thakur PK, Chouksey A, Aggarwal SP (2021) Identification of flash-floods-prone river reaches in Beas river basin using GIS-based multi-criteria technique: validation using field and satellite observations. *Nat Haz* 105(4):1–23
- Sivapalan M, Takeuchi K, Franks SW, Gupta VK, Karambiri H, Lakshmi V, Liang X, McDonnell JJ, Mendiondo EM, O'Connell PE, Oki T, Pomeroy JW, Schertzer D, Uhlenbrook S, Zehe E (2003) IAHS decade on predictions in ungauged basins (PUB), 2003–2012: shaping an exciting future for the hydrological sciences. *Hydrol Sci J* 48(6):857–880
- Strahler AN (1957) Quantitative analysis of watershed geomorphology. *Trans Am Geophys Union* 38:913–920
- Subramanya K (2013) *Engineering Hydrology*. McGraw-Hill Education (India) Private Limited. New Delhi, pp 534
- US-SCS (1986) *Urban hydrology for small watersheds*. Technical Release TR55, United States Soil Conservation Service (US-SCS), Washington DC, USA.
- USACE-HEC (2000) *Hydrologic Modeling System HEC- HMS: Applications Guide*. CPD-74C. US Army Corps of Engineers (USACE), Hydrologic Engineering Center (HEC), Davis, California, pp 108
- van Emmerik T, Mulder G, Eilander G, Piet M, Savenije H (2015) Predicting the ungauged basin: model validation and realism assessment. *Front Earth Sci* 3:62. <https://doi.org/10.3389/feart.2015.00062>
- Wagner T, Wheeler HS (2006) Parameter estimation and regionalization for continuous rainfall-runoff models including uncertainty. *J Hydrol* 320(1-2):132–154
- Yilmaz AG, Imteaz MA, Ogwuda O (2012) Accuracy of HEC-HMS and LBRM models in simulating snow runoffs in upper Euphrates basin. *J Hydrol Eng ASCE* 17(2):342–347
- Zhang Y, Vaze J, Chiew FH, Li M (2015) Comparing flow duration curve and rainfall-runoff modelling for predicting daily runoff in ungauged catchments. *J Hydrol* 525:72–86
- Zekele DG, Langon S (2020) Selection of appropriate loss methods in HEC-HMS model and determination of the derived values of the sensitive parameters for un-gauged catchments in Northern Ethiopia. *Int J River Basin Manag* 18(1):127–135
- Zekele DG, Melesse AM (2018) Applicability of a spatially semi-distributed hydrological model for watershed scale runoff estimation in Northwest Ethiopia. *Water* 10(7):923
- Springer Nature or its licensor (e.g. a society or other partner) holds exclusive rights to this article under a publishing agreement with the author(s) or other rightsholder(s); author self-archiving of the accepted manuscript version of this article is solely governed by the terms of such publishing agreement and applicable law.